

Appendix A

Photon Statistics and “Peaking Up” the Experiment”

In this appendix, I will discuss some of the details of the cycling transition ($|\downarrow\rangle \rightarrow |2p\ ^2P_{3/2}\rangle$). The statistics of the photons from this transition provide a sensitive guide to various aspects of the experiment. So, I will try to provide a recipe for “peaking up” the experiment, as well as discuss some of the limits to the cycling transition.

Basically, the peaking up based on the photon statistics falls into two categories: those methods based on the average number of photons detected per experiment (i.e. the mean count rate) and those based on the histogram of photon numbers per experiment. I shall deal with these in order. First, I will catalogue the various peak-up procedures based on average photon number, and then I will discuss what information can be gleaned from the histograms, as well as discussing the limit of the cycling transition’s quantum efficiency for discriminating $|\downarrow\rangle$ from $|\uparrow\rangle$ (due to off-resonant transitions from $|\uparrow\rangle$ into the cycling transition).

A.1 Peaking Up the Experiment With the Mean Photon Number

To recap, the typical experiment lasts anywhere from 0.5 – 1ms. At the end of each experiment, we turn on the Blue Doppler beam for typically 200 μ s, and measure the number of photons collected by the photodetection system (which has an overall quantum efficiency of $\approx 10^{-3}$ due to detector efficiency and solid angle). Typically, we detect photons with the imager tube while loading the trap, then switch to the

photomultiplier tube for peaking up the experiment and for taking data. The pulses output by these detectors are sent to a scalar (Ortec Model #9349), which produces a current proportional to the count rate (# of photons detected per second). This current is then used to drive galvanometers. Although using needle dials to indicate the average count rate may strike some as old-fashioned, this is, in fact, a very useful tool, as it seems to be the easiest way for people to assimilate the information. In particular, it is *much* easier to determine the maximum count rate while peaking up using the needle dials than using a digital count rate indicator. The time constant of the scalar is adjustable. We typically use a time constant of 0.3 s.

All the following peak-ups should be performed with the Blue and Red Doppler beams on continuously, and with the Raman and Repumper beams off (i.e. blocked!). Note that, if the Repumper beam is going into the trap, it will be impossible to peak up the Doppler beam lines, as the count rate becomes very “jumpy.”

After loading an ion and centering it in the imager tube, the first task is to maximize the count rate by adjusting the Doppler beam input lens. To do this, block the Repumper beam line and the Red Doppler, and maximize the count rate. Next, set the Blue Doppler polarization. With the Red Doppler still blocked (or, if the ion is flakey without the Red Doppler, attenuated to well below the saturation intensity), iterate between adjusting the angle and orientation of the quarter-wave plate, and adjusting the currents in the \mathbf{B} field shim coils. This procedure aligns the wave vector of the Doppler beam with the magnetic field.

Once the Blue Doppler beam is adjusted, let the Red Doppler in again (or, if it had only been attenuated, remove the attenuation). Unplug one of the shim coil current supplies. The count rate should drop, since the polarization has been effectively degraded. Then adjust the Red Doppler input beamsplitter to maximize the count rate.

In order to peak up the Repumper, it is usually best to turn Raman cooling on, then disable the Raman probe. The count rate should be considerably lower (20-30%)

lower than before Raman cooling was turned on. Next, allow the Repumper beam into the trap, and maximize the count rate. It is often useful to observe the photon number histogram (see below) to ensure that one has the Repumper beam position optimized.

A.2 Photon-Number Histograms

The histogram of the distribution of detected fluorescence photons is produced on the PC. A variable number of experiments are binned together (typically, 1000), and the resulting histogram is displayed on-screen. In addition, the mean number and the variance are calculated for the binned experiments and displayed. The variance should be exactly 1.00 for a Poisson distribution (which is the expected distribution). In practice, the number varies between 0.97 and 1.08 when 1000 experiments are binned together. If the variance creeps up much beyond 1.10, then something is wrong (usually, it's a problem with intensity or frequency fluctuations on the Doppler laser).

It is also useful to set a discriminator between $|\uparrow\rangle$ and $|\downarrow\rangle$ in terms of the number of photons received per experiment. The program calculates the percentage of experiments in which a number of photons corresponding to $|\uparrow\rangle$ was received, and displays this information as well. In practice, due to background light, scatter off the trap electrodes, and the limitation of the cycling transition in ${}^9\text{Be}^+$, the discriminator is usually set such that experiments in which two or less photons are received are binned as $|\uparrow\rangle$, and those in which more photons are received are binned as $|\downarrow\rangle$. The “limit” mentioned above is due to off-resonant pumping of population in $|\uparrow\rangle$ into the cycling transition, and will be further explained below.

In practice, a canonical $|\downarrow\rangle$ state is that which results from optical pumping at the beginning of the experiment. A canonical $|\uparrow\rangle$ state is produced by starting out in $|\downarrow\rangle$ and applying a π -pulse on the co-propagating carrier. With the discriminator set to two photons, $|\uparrow\rangle$ produces counts in the “ $|\downarrow\rangle$ ” channel 2-4% of the time. A $|\downarrow\rangle$ state typically produces no counts in the “ $|\uparrow\rangle$ ” channel. Typical histograms for

$|\downarrow\rangle$ and $|\uparrow\rangle$ are reproduced in Fig. A.1(a). Fig. A.1(b) shows a typical carrier Rabi flopping curve with photon number histograms shown for several interesting parts of the curve. In particular, note that the photon distribution for $\frac{1}{\sqrt{2}}(|\downarrow\rangle + |\uparrow\rangle)$ is the appropriately weighted sum of the $|\downarrow\rangle$ and $|\uparrow\rangle$ (Poissonian) histograms, rather than being a Poissonian at the average of the $|\downarrow\rangle$ and $|\uparrow\rangle$ average photon numbers.

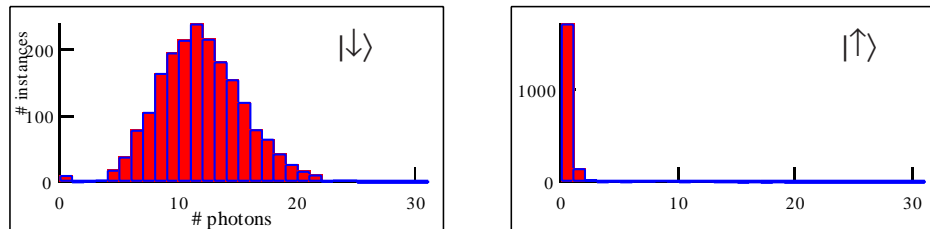
A.2.1 Discrimination Limits: Off-Resonant Pumping

The 2-4% “leak” of $|\uparrow\rangle$ into $|\downarrow\rangle$ bins is due to the finite hyperfine splitting of ${}^9\text{Be}^+$: the linewidth of the $2p^2P_{3/2}$ level is 19.4 MHz while the hyperfine splitting is only 1.25 GHz. Thus the state $|\uparrow\rangle$ occasionally scatters photons, rather than being truly dark — indeed, once $|\uparrow\rangle$ scatters a photon, it is likely that it will end up in $|\downarrow\rangle$, and hence participate in the cycling transition.

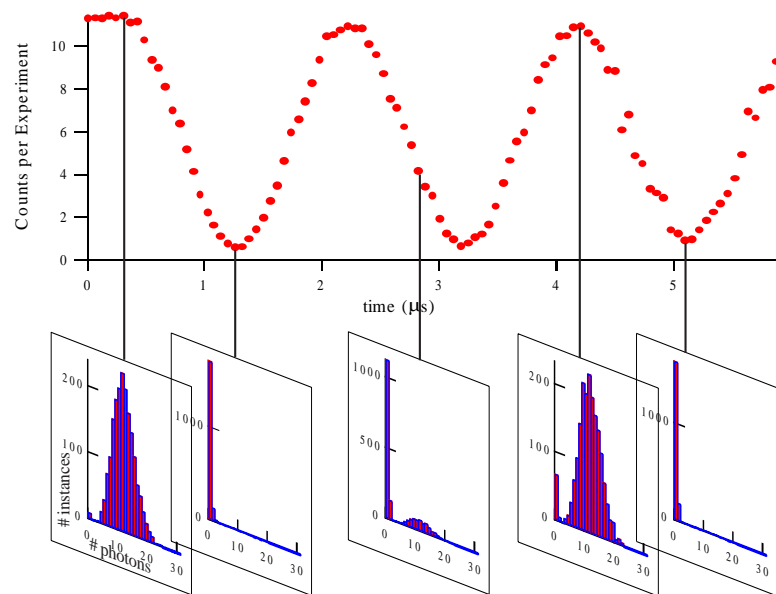
If the ion is in $|\downarrow\rangle$, then the photon number distribution is truly Poissonian, with $\bar{m} = \bar{m}_0 = \zeta\beta_2 t_{DG}$, where β_2 is the scatter rate in $|\downarrow\rangle$, t_{DG} is the length of the detection time gate, and ζ is the detection efficiency ($\zeta \approx 8 \times 10^{-3}$). The challenge is to calculate the photon number distribution if the ion is in $|\uparrow\rangle$ at the beginning of t_{DG} . In this case, the photon distribution is a spike at $\bar{m} = 0$ for some time t_p (related to the scatter rate β_2 due to off-resonant transitions) until the ion enters the cycling transition, at which point the photon distribution becomes a Poissonian with $\bar{m} = \bar{m}_0(1 - \frac{t_p}{t_{DG}})$. The complication occurs because t_p , being related to the excited state lifetime, is a random variable.

To be more quantitative, let

$$\beta_1 = \frac{\frac{I}{I_S} \frac{1}{2\tau}}{1 + \frac{I}{I_S} + 4 \left(\frac{\omega_0 + \delta}{\gamma} \right)^2} \approx \frac{\frac{I}{I_S} \frac{1}{2\tau}}{1 + \frac{I}{I_S} + 4 \left(\frac{\omega_0}{\gamma} \right)^2} \quad (\text{A.1})$$



(a)



(b)

Figure A.1: (a) Photon number histograms for $|\downarrow\rangle$ and $|\uparrow\rangle$. 1000 experiments were binned together for each histogram, and Detection Gate was $200\ \mu\text{s}$. The counts in the nonzero $|\uparrow\rangle$ bins are due to background and to off-resonant pumping of $|\uparrow\rangle$ population into the cycling transition. (b) Carrier flopping curve with photon number histograms at select points. Note that halfway down the flopping curve, when the ion is in $1/\sqrt{2}(|\downarrow\rangle + |\uparrow\rangle)$, the photon distribution is the sum of the $|\downarrow\rangle$ and $|\uparrow\rangle$ distributions, and not a Poissonian centred at the average of the $|\downarrow\rangle$ and $|\uparrow\rangle$ average count rates.

be the base off-resonant scatter rate of photons when the atom is in $|\uparrow\rangle$ (neglecting the laser polarization and atomic matrix elements, for the moment) and

$$\beta_2 = \frac{\frac{I}{I_S} \frac{1}{2\tau}}{1 + \frac{I}{I_S} + 4 \left(\frac{\delta}{\gamma}\right)^2} \quad (\text{A.2})$$

be the scatter rate of photons when the atom is in $|\downarrow\rangle$ (i.e. the cycling transition scatter rate). In these equations, τ is the $2p^2P_{3/2}$ lifetime and γ its linewidth, I is the laser intensity, I_S is the saturation intensity, and δ is the detuning from resonance. (In practice, δ will be negative to allow laser cooling with the Doppler beams.)

Now, the atomic levels of interest, along with the appropriate transition strengths, are shown in Fig. A.2(a). Eliminating the excited state levels, we get the simplified level structure of Fig. A.2(b), which guides us in writing down the following rate equation for the population in $|\uparrow\rangle$:

$$\begin{aligned} \dot{P}_\uparrow &= - \left[\frac{1}{6}\beta_1 + \frac{5}{24}\beta_1 \frac{\frac{1}{18}\beta_2}{\frac{1}{18}\beta_2 + \frac{5}{24}\beta_2} \right] P_\uparrow \\ &= \frac{4}{19}\beta_1 P_\uparrow. \end{aligned} \quad (\text{A.3})$$

Thus, $P_\uparrow(t) = P_\uparrow(0)[1 - \exp(-\frac{4}{19}\beta_1 t)]$. Of course, this equation reflects the *average* dynamics of $|\uparrow\rangle$: in a single experiment, the atom follows a probability distribution of decay times. Guided by Eq. (A.3), we write:

$$p(t_p) = \frac{1}{\tau_p} e^{-\frac{t_p}{\tau_p}}, \quad (\text{A.4})$$

where $\tau_p = \frac{19}{4\beta_1}$.

To reiterate, we see no photons until the atom off-resonantly pumps into the cycling transition at (random) time t_p . Then, we see a Poissonian distribution with $\bar{m} = \bar{m}_0(1 - \frac{t_p}{t_{DG}})$. Thus, the probability distribution for the number of photons observed in an experiment may be written as the conditional probability distribution:

$$P(m|\bar{m}) = \frac{e^{-\bar{m}} \bar{m}^m}{m!}. \quad (\text{A.5})$$

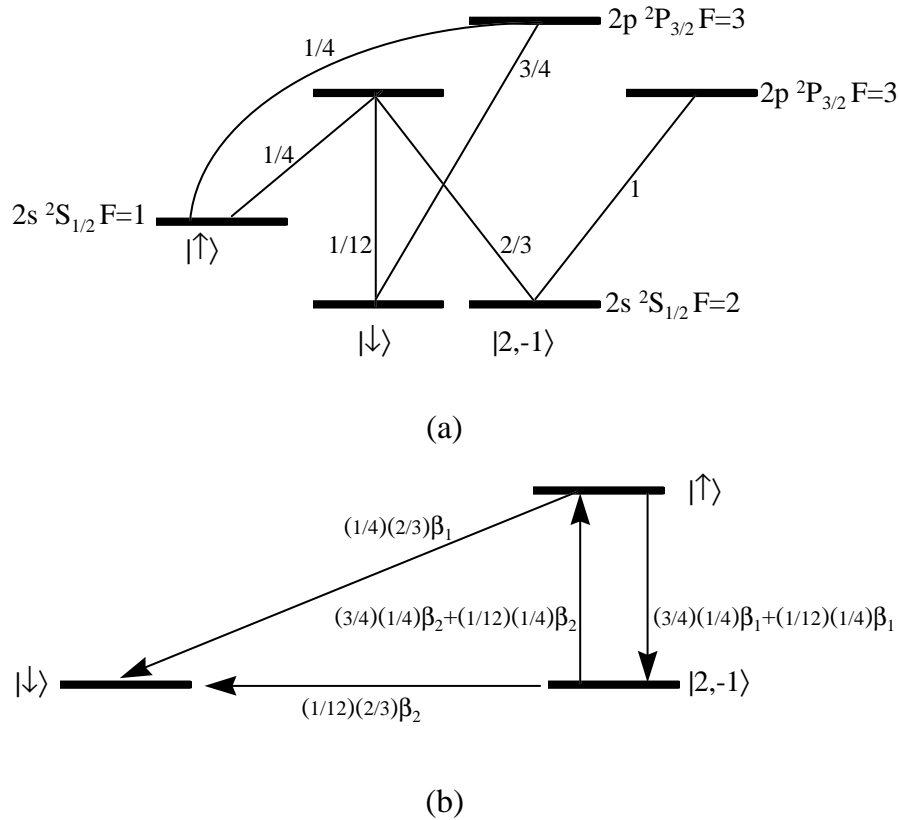


Figure A.2: (a) Relevant energy levels in ${}^9\text{Be}^+$ for discussing off-resonant pumping of $|\uparrow\rangle$ population into the cycling transition. The numbers are the relative transition strengths. See Appendix B for a complete diagram of transition strengths. (b) Simplified effective level diagram, showing the various rates of population transfer.

It follows that the probability of observing m photons in an experiment is given by:

$$P(m) = \int P(m|\bar{m})\rho(\bar{m})d\bar{m}, \quad (\text{A.6})$$

where $\rho(\bar{m})$ is the probability distribution for \bar{m} (due to the random nature of t_p).

In order to calculate $\rho(\bar{m})$, we can write down the cumulative distribution of \bar{m} :

$$F_M(\bar{m}) = \text{Prob.}(M \leq \bar{m}) = \int_{\{t_p: M(t_p) < \bar{m}\}} p(t_p) dt_p, \quad (\text{A.7})$$

where M is the number of photons detected. From the expression $\bar{m} = \bar{m}_0(1 - \frac{t_p}{t_{DG}})$, we may rewrite the domain of integration as $t_p > (1 - \frac{\bar{m}}{\bar{m}_0})t_{DG}$. Putting this into the

above integral, and plugging in for $p(t_p)$ from Eq. (A.4), we may evaluate the integral:

$$\begin{aligned} F_M(\bar{m}) &= \int_{(1-\frac{\bar{m}}{\bar{m}_0})t_{DG}}^{\infty} \frac{1}{\tau_p} e^{-\frac{t_p}{\tau_p}} dt_p \\ &= e^{-\frac{t_p}{\tau_p}(1-\frac{\bar{m}}{\bar{m}_0})}. \end{aligned} \quad (\text{A.8})$$

Then, we may calculate the probability distribution for \bar{m} :

$$\rho(\bar{m}) = \frac{\partial F_M(\bar{m})}{\partial \bar{m}} = \frac{t_p}{\bar{m}_0 \tau_p} e^{-\frac{t_p}{\tau_p}(1-\frac{\bar{m}}{\bar{m}_0})} + e^{-\frac{t_p}{\tau_p}} \delta(\bar{m}). \quad (\text{A.9})$$

The δ -function is due to the discontinuity of the integral at $t_p = 0$.

Finally, plugging back into Eq. (A.6), we have that the probability of observing m photons in a given experiment, given that we start out in $|\uparrow\rangle$, is:

$$P(m) = e^{-\frac{t_{DG}}{\tau_p}} \delta_{m,0} + \frac{t_{DG} e^{-\frac{t_{DG}}{\tau_p}}}{\tau_p \bar{m}_0 m!} \int_{0+\epsilon}^{\bar{m}_0} e^{(\frac{t_{DG}}{\tau_p \bar{m}_0} - 1)\bar{m}} \bar{m}^m d\bar{m}. \quad (\text{A.10})$$

With some minor tweaking, the integral can be put into the form of an incomplete Gamma function ([72]§6.5), and we finally have:

$$P(m) = e^{-\alpha \bar{m}_0} \left[\delta_{m,0} + \frac{\alpha}{(1-\alpha)^{m+1}} P(n+1, (1-\alpha)\bar{m}_0) \right], \quad (\text{A.11})$$

where $\alpha = \frac{t_{DG}}{\tau_p \bar{m}_0}$ and $P(m+1, (1-\alpha)\bar{m}_0)$ is the incomplete Gamma function. Note that this function is the cumulative distribution for the Chi-square distribution.

The important fact to draw from Eq. (A.11) is that $P(0)$, which should ideally be equal to 1, is given by $P(0) = \exp(-\frac{t_{DG}}{\tau_p} \bar{m}_0) = e^{-\alpha \bar{m}_0}$, where $\alpha \approx \frac{4}{19\zeta} (\frac{\gamma}{2\omega_0})^2$. For ${}^9\text{Be}^+$, we have that $\alpha \approx \frac{1.35 \times 10^{-5}}{\zeta}$. This is the fundamental limit to the accuracy of discriminating $|\uparrow\rangle$ from $|\downarrow\rangle$. Thus, with $\zeta \approx 8 \times 10^{-3}$, we have $P(0) \approx 0.98$ under typical operating conditions, rather than $P(0) = 1$. Fig. A.3 shows photon number histograms for optimum conditions and for the case in which the Blue Doppler intensity is high enough that power broadening exacerbates the leak out of $|\uparrow\rangle$.

In terms of the cycling transition, ${}^9\text{Be}^+$ is actually one of the worst alkali-like ions, due primarily to its small hyperfine splitting. For example, $\alpha = \frac{3.7 \times 10^{-7}}{\zeta}$ for Cd^+

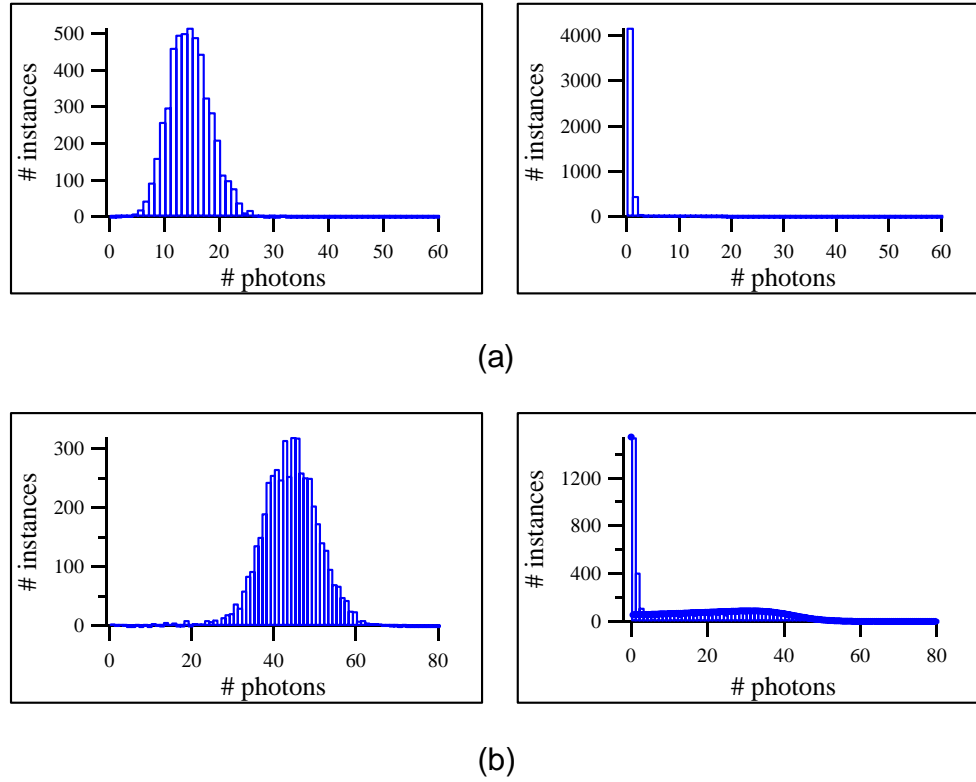


Figure A.3: Photon number histograms versus power broadening. (a) Photon number histograms for optimum Blue Doppler intensity. In particular, note that the number of photons in “ $|\downarrow\rangle$ ” channels for the $|\uparrow\rangle$ state is only 6% of the total. (b) Photon number histograms when the Blue Doppler intensity is large enough that power broadening pumps population from $|\uparrow\rangle$ into the cycling transition. 59% of the counts for the state $|\uparrow\rangle$ are in “ $|\downarrow\rangle$ ” channels. The dots are a fit to Eq. (A.11). The fit gives 3188 as the total number of instances (the actual number is 5000 — this reflects the excess experimental counts in Channels 1 and 2, due to background), $\alpha = 0.017$, and $\bar{m} = 43$ (compare with the average photon number in the $|\downarrow\rangle$ histogram).

on the $S_{1/2} \leftrightarrow P_{3/2}$ cycling transition, and $\alpha = \frac{5.3 \times 10^{-7}}{\zeta}$ for $^{199}\text{Hg}^+$ on the $S_{1/2} \leftrightarrow P_{1/2}$ cycling transition. For these ions, the cycling transition thus allows almost perfect discrimination between the bright and dark states, for the photon detection efficiency available in our experiment.

A.2.2 Fine-Tuning the Resonant Beam Intensities

The histograms can be used to fine-tune the Blue Doppler, Red Doppler and the Repumper intensities, and are also useful in setting the Repumper beam position. To set the Blue Doppler intensity, vary the attenuation (rf and optical) in the Blue Doppler line to get as many counts as possible per experiment without exacerbating the off-resonant pumping of $|\uparrow\rangle$ into the cycling transition. In practice, with our solid angle, a $200\ \mu\text{s}$ Detection Gate, and the Blue Doppler beam detuned roughly halfway down the resonance curve (i.e. 10 MHz detuned), this corresponds to $\bar{m} \approx 10$ for $|\downarrow\rangle$. This gives less than 2% discrimination error between $|\uparrow\rangle$ and $|\downarrow\rangle$.

The Red Doppler intensity may be set in much the same way. If the intensity is too low, then optical pumping is not efficient, and state preparation suffers. So, for example, if we drive a co-propagating carrier π -pulse to prepare the state $|\uparrow\rangle$ then any population which was left in $|\uparrow\rangle$ after optical pumping gets transferred to $|\downarrow\rangle$. Rather than producing a dark state, we produce a mixture of photon counts corresponding to $|\uparrow\rangle$ and $|\downarrow\rangle$. On the other hand, if Red Doppler is too intense, then the efficiency of optical pumping becomes much more sensitive to imperfections in the Red Doppler polarization due to off-resonant pumping *out* of $|\downarrow\rangle$.

Finally, the histograms may be used to line up the Repumper beam on the ion. This beam is typically wider than the Blue and Red Doppler beams before the input lens. Thus it is more tightly focussed at the ion, and so is harder to align. Also, this beam is less intense than the Doppler beams. However, once Raman cooling is turned on, the multiple recyclings from $|\uparrow\rangle$ to $|\downarrow\rangle$ produce a large probability that the ion will fall into the $2s\ ^2S_{1/2}F = 2, m_F = -1$ state. If we try to make the state $|\downarrow\rangle$ with Raman cooling on and the Repumper off then we get a pile-up of counts in the first few bins of the photon number histogram. Fig. A.4(a) illustrates this (compare with Fig. A.4(b), where the Repumper beam is aligned on the ion). Note that, with the

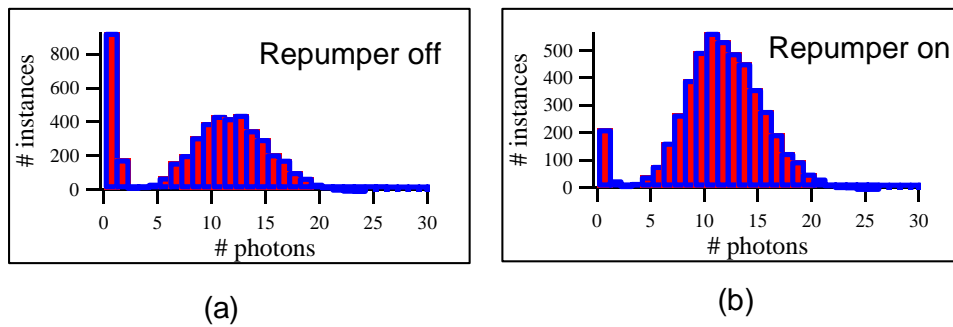


Figure A.4: (a) Photon number histogram with the ion nominally in $|\downarrow\rangle$, but Raman cooling on and no Repumper. 23% of the counts fall in bins which correspond to $|\uparrow\rangle$. (b) Photon number histogram for the same conditions as in (a), but with the Repumper aligned on the ion. Now, only 5% of the counts fall in channels corresponding to $|\uparrow\rangle$.

Repumper blocked, 23% of the counts for a nominal $|\downarrow\rangle$ state fall into the first three channels.

In order to peak up the Repumper, sit off-resonance with the Probe oscillator (or turn the Probe off), and maximize the count rate (looking at the needle gauge) by playing with the input optics for the Repumper beam line. Once the Repumper is optimized, there shouldn't be more than 4-8% of the counts in the first three bins of the photon number histogram.